Design and construction of a stepping shape memory actuator for driving a variable camber aircraft wing

D. Reynaerts[1] W. Van Moorleghem[2] H. Van Brussel[1]

[1] Katholieke Universiteit Leuven
Mechanical Engineering Dept.
Celestijnenlaan 300B, B-3001 Heverlee
domi@ieee.org

[2] Advanced Medical Technologies (AMT)
R&D Dept.
Daelemveld 1113, B-3540 Herk-de-Stad
wilfried@amtbe.com

Abstract

This paper describes the design and development of a wing flap with variable camber in order to have an optimal lift under all flight conditions. Such a variable flap reduces the fuel consumption considerably and thus enlarges the action radius of the aeroplane. In order to realise the variable camber, the trailing edge is deflected over an angle of ± 5°. Shape memory alloy (SMA) material is selected to actuate the variable flap because of its high power to mass and power to volume ratios. A stepping concept has been chosen to optimise efficiency.

1. Introduction

This paper describes the design and development of a wing flap with variable shape (or camber) in order to have an optimal lift under all flight conditions. The aim is to therefore to deflect the trailing edge of the wing flap (Figure 1). This engineering problem has already been addressed in various ways, implementing an active material being perhaps the most prominent one.

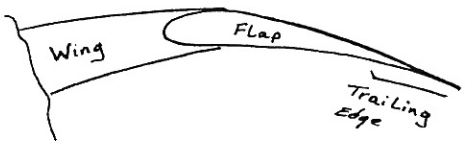

Figure 1: Concept of a variable camber wing

1.1. Previous work on active materials

Recently, a lot of work is done on the research and development of smart structures or materials with embedded Shape Memory Alloy (SMA) actuators. This field, however, is still very much at the research stage and many system, control and fabrication problems remain to be solved. Also, an adequate model should be built for the SMA material itself and for its interaction with the host composite material for every specific application.

Lagoudas *et al.* [1] modeled a cylindrical rod with a single off-axis embedded SMA fibre under uniform pre-strain. Bo *et al.* [2] continued this research and compare the results of the analytical model, of a finite element model, and of experiments. Beauchamp *et al.* [3] proposed a design for an adjustable camber foil to control the flight of hydrodynamic or aerodynamic vehicles. Dittrich [4] presents the work done by Deutsche Aerospace AG on changing the shape of wing structures with integrated SMA actuators. Paine *et al.* [5] describe the use of SMA hybrid composite materials for high-pressure vessels. High-pressure composite pressure vessels can reduce the size and weight of fuel, hydraulic and auxiliary systems in aerospace applications.

Vibration control, which may also be used for structural acoustic control, can be accomplished with SMA hybrid composite materials by employing 'Active Modal Modification'. The modal response can be tuned by heating the SMA fibres to change the stiffness of the structure. Rogers *et al.* [6,7] describe experimental studies performed to determine the extent of structural modification made possible with NiTi-graphite-epoxy hybrid composite systems.

These strain control applications, like vibration control, and the superelastic applications, like increased impact damage resistance, seem to be at a stage where the practical implementation is already closer as for the shape control implementation that is envisaged here. This is especially the case when the shape control actuator works under external load conditions or under partial actuation conditions and in continuous mode operation. This continuous mode operation implies also a very low energetic efficiency.

1.2. Application of an integrated solution

There are two possible ways to design an integrated structure for the flap with variable camber. The first solution is to embed the SMA material in a matrix material in order to make an actuated flexible skin. The second solution consists of integrating SMA wires in a flexible structure so that the entire trailing edge is actuated. Dittrich [4] followed this approach in his research. Following sections discuss both alternatives.

An actuated flexible skin

An actuated flexible skin surely offers the most compact solution and at first sight also the simplest one. Contraction of the skin on top of the flap deflects the trailing edge in the upward direction, and contraction of the skin at the bottom in the downward direction. The major problems when integrating the SMA wires in the flexible skin are listed below.

- The control of a lot of parallel SMA wires still remains an unsolved problem. Not all the SMA wires contract at the same moment due to local variations of temperature, supply current, length of the SMA wire, or a difference in extension after the previous contraction. The non-synchronised contraction increases the stress in the SMA wires that contract first. This decreases the SMA material lifetime considerably and in the worst case it can even lead to failure of the system.
- The full contraction of the SMA material, which is around 3 %, can not be entirely used since the composite material does not permit such a strain.
- The thermal and electrical isolation of the matrix from the SMA wires is another problem, especially when considering the very cold airflow over the flap.
- The attachment of every single SMA wire is a production or assembly problem, since every wire must have the same pre-tension. The only maintenance operation possible is a replacement of the complete structure.
- The only way to achieve an active shape control is to continuously heat the SMA material when a deflection of the trailing edge is needed. This option, however, should be rejected because of the very low efficiency and large energy consumption. Allowing cooling of the SMA while the structure remains deformed requires a decoupling between SMA and structure.
- A similar unlocking system is needed in case the aeroplane is on the ground and the temperature rises above the transformation temperature of the SMA material.
- Because of the required structural flexibility, the stiffness of the entire trailing edge is low and the danger of flutter occurs.

An integrated flexible trailing edge structure

Dittrich [4] describes the work done by Deutsche Aerospace AG in this area. The aim of the design is to develop a flexible trailing edge that is actuated by integrated SMA actuators (Figure 2). The flap skin is continuous, without gaps and discontinuities, and is deflected in a smooth and continuous way. As in the previous section, the operation of the actuators is antagonistic. In order to choose the best design for the flexible structure (glass fibre reinforced polymer) several design concepts are modelled with finite elements. The SMA wires provide the stiffness of the entire structure.

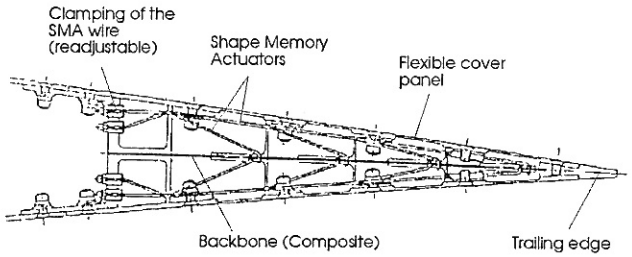

Figure 2: An integrated flexible structure.

However, Dittrich [4] reports following problems with this design:

- Still, the most optimal design for the flexible structure generates a strain of 3.5 to 4 % in the composite material.
- Because of the hysteresis in the SMA material, some control problems may occur.
- The operational temperature of the SMA actuators should be above the maximal temperature of the aeroplane (above +90 °c) in order to avoid uncontrolled contraction of the actuators. This problem occurs because of the deficiency of an unlocking mechanism.
- The attachment of the SMA wires to the composite structure remains a problem since it is difficult to weld, braze, or solder them. In this case also mechanical clamping is difficult.

The design described above solves some of the material problems mentioned before, since the SMA wires are not integrated in the composite material itself. However, most of the design, the control, the manufacture, and the maintenance problems remain unsolved, even with this concept.

It was concluded that the present technical state of integrated SMA composites does not allow the use of a composite material with integrated SMA actuators. Although a flexible structure with integrated SMA actuators solves some of the material problems, it does not offer a satisfactory solution. Therefore, it was decided to design an alternative solution consisting of a separate actuator unit that can be integrated in the existing flap structure.

2. System Design

The design described in this paper has been made for the inner most part of the trailing edge. For this part, an actuator unit is designed in one particular section of the flap. The shape and dimensions of this section are

retrieved from a commercial aeroplane. The general concept is a linear actuator driving a force transmission mechanism to deform the trailing edge of the flap. The linear actuator proposed is an inchworm [8] type of actuator making steps of about 12 mm. Each step corresponds to trailing edge deflection of 1°. The total deflection range is 5° up and down deflection (10 steps). A first section of describes the force transmission system. A second section concentrates on the inchworm actuator.

2.1. The force transmission system

The integration of the actuator and the transmission in the flap is severely restricted by geometrical constraints and was mainly done with a trial and error method. The kinematic equations of the cam-follower system and the vertical lever with hinge joint were programmed parametrically in Matlab. This model provides the necessary dimensional data when repositioning parts of the mechanism. In order to have a good three-dimensional understanding of the design, a solid model of the mechanism was made in the CAD-program Unigraphics. Figure 3 shows the force transmission system integrated in the rear part of the flap.

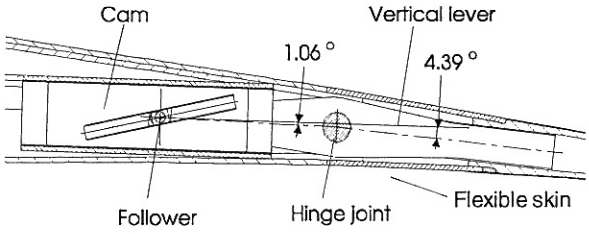

Figure 3: Integration of the force transmission system.

The aluminium cam slides in an aluminium housing that is covered with a low friction surface coating. The cam has a sleeve in which the follower operates and which is also covered by a low friction surface coating. The follower has a rectangular shape with rounded edges in order to have a larger contact surface. It is made of steel because of the high forces it transmits. The inclination of the sleeve determines the magnitude of the 'horizontal' motion of the cam. This magnitude should be limited to avoid a collision with the hinge joint. Moreover, the inclination of the sleeve determines the force reduction ratio and also weather the cam is self-locking or not. A self-locking cam is preferable for safety reasons. In the proposed design, the angle of the sleeve is 13.32°. In order to have perfect discrete steps of 1° for the trailing edge, the sleeve should be slightly curved since the follower makes a rotational motion around the hinge joint. The maximal positioning error resulting from a straight sleeve approximation is only 0.033°. In the neutral position, the plane for mounting the housing and the cam (and also of the inchworm actuator) makes an angle of 1.06 ° with the plane containing the follower and the axis of the vertical lever. This is necessary because of the shape of the rear flap part. Note that the only connection between the sliding trailing edge and the flap structure are the two flexible skins covering the mechanism. As this would lead to an uncontrolled motion of the trailing edge (e.g. by air pressure variations), an extra mechanism is required (see bleow).

The vertical lever consists of two symmetrical beams that are mounted on each side of the cam (Figure 4). This allows a symmetrical force transmission without any deformations due to asymmetric loading of components. Both beams are connected by a heavy steel shaft that at the same time is the axle of the hinge joint. The trailing part of the lever is sliding in the trailing edge. In neutral position, the slider in the trailing edge has an inclination 4.39 ° with respect to the mounting plane of the actuator. Again, this is due to the shape of the rear flap part.

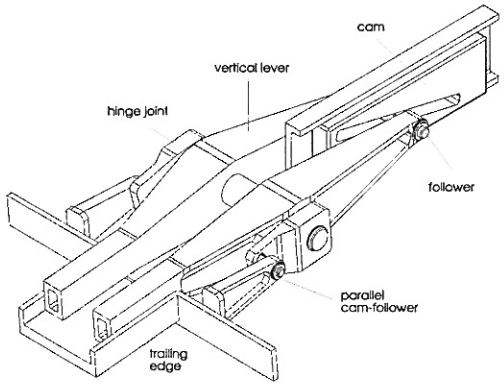

Figure 4: The entire force transmission system (open, top view).

The follower is mounted between the two beams by means of plain bearings. These bearings are much more compact than ordinary ball bearings, but have the disadvantage of more friction. However, this is of minor importance since the rotational speed is very limited. For this reason, also the axle of the hinge joint is mounted by means of two plain bearings. Note that all plain bearings used in this design are flanged so that they can also take axial forces. At the other end of the lever, the beams slide into the trailing edge. Again, a surface coating provides the required low friction coefficient.

The parallel cam-follower system (see above) that provides the controlled motion of the trailing edge and actively adapts the distance from the trailing edge to the front part of the flap is shown in Figure 5. In this case, the cam is fixed to the flap structure and is integrated in the aluminium bearing blocks of the hinge joint. A rectangular follower in steel slides in the sleeve and is connected by a hinge joint to a beam. This beam is in its turn fixed to the trailing edge. This shape is such that the

distance from the flap body to the trailing edge is adapted in a way that the flexible skin only bends without elongating in axial direction. The obtained 'S'-curve is approximated by a straight line with an angle of 58.59° with respect to the trailing edge. This enables the use of a rectangular follower. This approximation induces an axial strain in the flexible skin of maximally 0.0866 %.

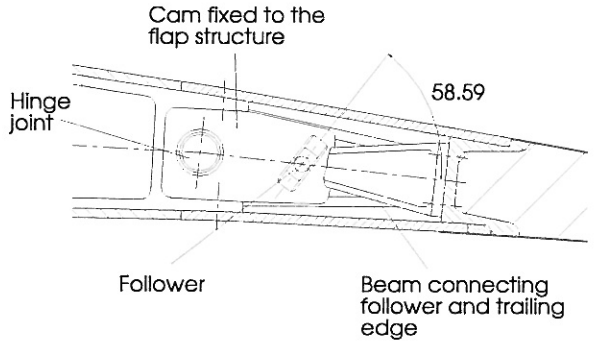

Figure 5: The parallel cam-follower system.

2.2. Description of the inchworm actuator

Figure 6 shows the entire section of the flap. At the right side the force transmission system is integrated in the flap. Starting from the right side, an aluminium ground plate is mounted up to the front of the flap. This plate serves to mount the inchworm actuator.

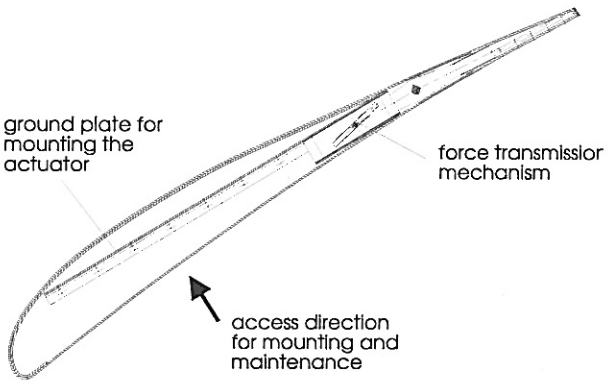

Figure 6: Flap section with force transmission system.

For maintenance purposes it is necessary to be able to check the inchworm actuator without dismounting it. For this reason it is mounted upside-down in the flap. Figure 7 shows the entire actuating mechanism, mounted in this upside-down position, without the surrounding flap structure. The total length of the mechanism is about 1m. The force transmission system (left side) is connected with the inchworm actuator (right side) by a simple steel beam.

Figure 8 shows a more detailed top view of the inchworm actuator. Both parts of the inchworm are mounted on a linear guide so that they can move independently. In between the two parts, four bias springs and the SMA wire are mounted. Note that the SMA wire is not drawn. Both parts have a locking mechanism.

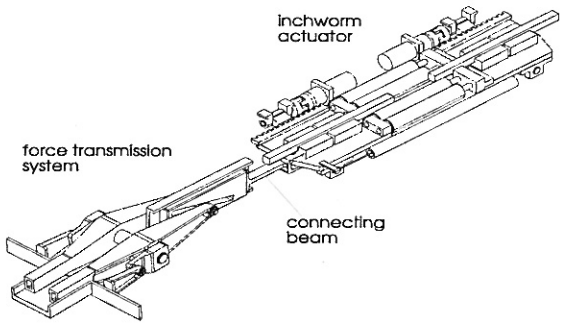

Figure 7: Entire actuating mechanism (open, top view).

The absolute position of the left part of the inchworm (and thus the deflection of the wing) is measured with a LVDT (Linear Variable Differential Transformer). Strictly spoken the LVDT is not necessary for operating the actuator because all necessary end positions are measured by microswitches. The LVDT can enhance the reliability of the device by providing an absolute reference measurement for the left slide of the inchworm and for the position of the trailing edge.

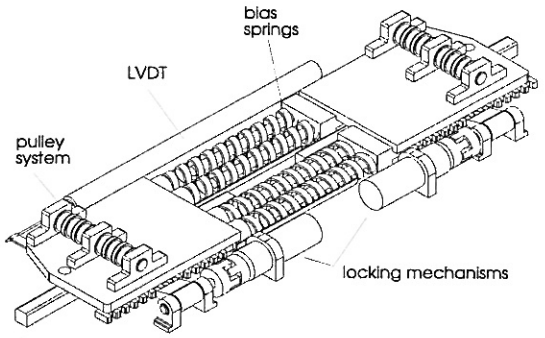

Figure 8: The inchworm actuator (open, bottom view).

Each part of the inchworm consists of an aluminium plate that is screwed on two slides of the linear guide. On this aluminium plate three support blocks are screwed to attach the steel shaft of the pulley system. The pulleys slide directly on the steel shaft. They are made in Ertalon 4.6 because of its good friction properties and of its high temperature resistance.

The locking mechanism consists on one side of a steel rack screwed on the corresponding slides of the actuator. The steel rack interacts with a kind of pinion that is actuated by an electrical motor. A hollow steel shaft supports the bias springs. The SMA wire is wound around the pulleys in such a way that there are twelve parts of the wire acting in parallel. A mechanical clamping system is

used for attachment of the SMA wires. All parts of the inchworm actuator described in this section do not contribute to the structural stiffness of the flap itself. For this reason all parts are mainly dimensioned by strength calculations.

3. Dimensioning of the SMA wire

This section calculates the required output forces of the actuator unit and dimensions the SMA wire. First, the external load on the inner most part of the trailing edge is calculated. By adding the torque due to the flexible skin bending and the estimated friction in the mechanism, the total torque is obtained. This total torque is transmitted in a net force for the actuator by the force transmission system. This allows dimensioning the bias springs and the SMA wire. Finally, this allows calculating the energetic efficiency.

The total air load F_{air} on the flap is in this case $F_{air} = 94800$ N. This leads to an air load F_{inner} on the inner part of the trailing edge of $F_{inner} = 7110$ N.

The torque T_{inner} on the inner part of the trailing edge is, therefore 1043 Nm to be delivered by two actuators. Taking into account friction and all requested safety factors (1.5) in the sliding transmission this gives an actuator torque $T_{act} = 900$ Nm and a net actuator force of $F_{pull} = 3100$ N.

During cooling of the wire, the force to be delivered by the bias spring can be split up in two forces with a different nature. F_{s1} is the force necessary to push back the cam. F_{s2} is the force necessary to stretch the SMA-wires from their austenitic state back to the (long) martensitic state. It is assumed that this stretching corresponds to a material stress $\sigma_{stretch} = 35$ N/mm^2. The stress in the SMA material when actuating the system is limited to $\sigma_{brut} = 100$ N/mm^2. This is considered to be a safe design value. Taking all this into account, the total actuator force $F_{act} = 5385$ N. This force is in fact an overestimation because of all safety factors included in the calculations. For the bias spring, it is proposed to take 4 springs with uncompressed length of 305 mm and a stiffness k_{spring} of 7 N/mm. Given that 4 springs act in parallel, the effective spring force will cover following range:

$$2884 \text{ N} \leq F_{eff\text{-}spring} \leq 3220 \text{ N}$$

This value is always larger than the required spring force for extending the actuator $F_{spring} = 2285$ N. Given this bias force, the effective force to be delivered by the actuator will cover following range (to be larger than the above required force for the actuator 5385 N):

$$5984 \text{ N} \leq F_{eff\text{-}act} \leq 6320 \text{ N}$$

This means that the minimal cross-section for the wire is raised to 63.2 mm^2. With 12 parallel SMA wires, this leads to a wire with section $A_{wire} = 5.5$ mm^2. The minimal total length of the SMA wire is then to 5400 mm. A contraction of 3% for this wire will result in a displacement of 13.5 mm, which is more than the required displacement of 12 mm. This means that the wire never will reach the fully austenitic state, which is favourable for the overall life-cycle behaviour

4. Energetic aspects

In this design, internal heating (based on Joule-effect) of the SMA is used. This method is preferable because it heats the material in a smooth and uniform manner. The proposed inchworm actuator contains 12 wires mechanically connected in parallel, but electrically acting in series. A pulley system is implemented to have an equal load (and thus equal transformation behaviour) on all wires. Taking into account clamping and connection systems, the total wire length will be $l_{wire} = 5.927$ m. Given the density of the SMA material, $\rho_{SMA} = 6500$ kg/m^3, the total mass of the SMA active element will be: $m_{wire} = 0.212$ kg. This value illustrates the tremendous potential of SMA materials in terms of power density.

Considering that the power supply voltage U = 28 V DC, the electrical specifications of the system can be determined. The current through the wire will then be I = 25.9 A and the power consumption only P = 725 W. The overall efficiency of the actuator can also be calculated. As the maximal heating times are found for an environment at –70 °C, the following calculations are based on this worst case situation. The electrical energy input necessary for heating the SMA wires is $E_{in} = 22040$ J. Various components contribute to this value.

The energy required to heat the active element from environmental temperature (-70 °C) to fully transformed state (A_s) is $E_{envas} = 15152.5$ J The energy for transformation, including heat losses to the environment is $E_{asaf} = 6888$ J. The total energy delivered by the actuator is $W_{act} = 73.8$ J.

The energy for compressing the spring is $W_{spring} = 36.6$ J. The useful work output of the inchworm actuator is then $W_{worm} = 37.2$ J. The efficiency of the transformation of the SMA material can be defined as follows:

$$\eta_{SMA} = W_{act} / E_{asaf} \cdot 100 = 1.1 \%$$

The overall efficiency of the inchworm actuator can be defined as follows:

$$\eta_{worm} = W_{worm} / E_{in} \cdot 100 = 0.17 \%$$

The work required to turn the lever over an angle of 1 degree is $W_{lever} = 15.7$ J. This means that the driving of the force transmission system to move the flap requires following energy or work input:

$$W_{cam} = W_{worm} - W_{lever} = 21.5 \text{ J}$$

This loss in fact also represents the safety factors included in the calculations. The real work output takes only in account the force to act against the air-load on the flap without any friction or elastic energy in the flexible skin $W_{inner} = T_{inner}/2 \cdot k_{safe} \cdot \pi/180 = 13.7$ J The energy lost in friction in the hinge, the parallel mechanism, the lever and due to the flexible skin will be: $W_{fric} = W_{lever} - W_{inner} =$ 2 J. This results in an overall efficiency of this type of actuation of :

$$\eta_{tot} = W_{inner} / E_{in} \cdot 100 = 0.062 \%$$

Figure 9 summarises all the above results in a Sankey-diagram. The overall efficiency of 0.062 % immediately explains that only an intermittent operation of the actuator can be allowed.

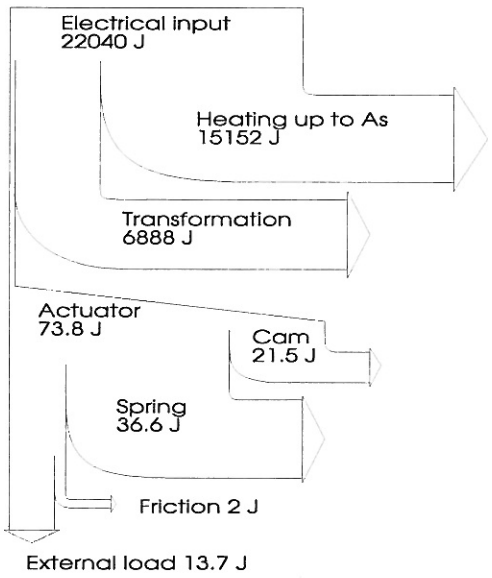

Figure 9: Sankey-diagram

Even if this efficiency is very low, the energy consumption of the actuation system is very low compared to the possible gain obtained by a reduction of the fuel consumption. The total energy input for 12 actuators, acting 20 times during a transatlantic flight will be $E_{totin} = 12 \cdot 20 \cdot E_{in} \approx 0.5\ 10^7$ J. If this would result in a reduction of fuel consumption of only 0.1 % on a total consumption of 100 ton fuel, the saved energy will be (given a specific energy of 40 MJ/kg):

$$E_{save} = 100\,000 \cdot 40\ 10^6 \cdot 0.001 = 4\ 10^{10} \text{ J}$$

This represents a gain factor of 800 times the consumed energy by using the proposed actuator mechanism for the smart wing.

5. Experimental set-up

The prototype mainly consists of five parts(Figure 10):

- a load including a lever mechanism transmitting a force equivalent to the air load on the lever of the proposed force transmission mechanism
- the cam-based force transmission system itself, converting the linear force of the actuator in a torque
- the inchworm actuator including the two locking mechanisms
- a set of air fans for cooling purposes
- a PC with a data-acquisition system and power amplifiers to drive the actuators (not on picture)

Compared to the design proposed above, mainly the lever arm to the trailing edge of the flap was changed. Also the parallel cam-follower system is not included. However, this system allows applying an equivalent load to the actuator and thus allows testing the performance of the inchworm actuator in realistic conditions. The air fans were added to decrease the cooling time for this set-up. As it is operating at room temperature and not at -40 or -70 °C, the cooling time would otherwise be too large. shows the equivalent load mechanism and the forces to be exerted to obtain a nominal load for the actuator. As calculated above, the actuator has to generate a torque $T_{act} = 900$ Nm. Because of the safety factor 1.5, the nominal torque for the actuator $T_{act\text{-}nom} = 600$ Nm. As shown on Figure 10, this torque can be obtained by hanging a mass of 82.6 kg at the left side of the mechanism.

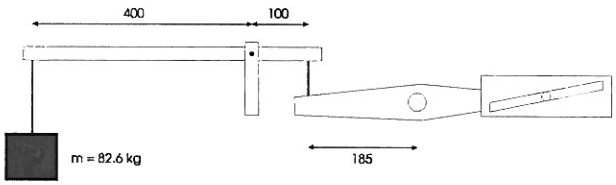

Figure 10: Equivalent load

Figure 11 shows a simplified schematic view of the control system for this prototype. The control system mainly consists of a PC that is equipped with a National Instruments AT-M10-16XE-50 data acquisition board. The applied board configuration enables 4 digital input channels (Dig_In), 4 digital output channels (Dig_Out), and 2 analog output channels (An_Out). The digital input channels are used to monitor the contracted (wiremin) or extended state (wiremax) of the actuator and to monitor the operation of the locking mechanisms. Due to the limited number of inputs, a NOR-function is applied to the output of the micro switches of the locking systems. In this way only a state transition can be monitored as the closed or open position can not be distinguished. Using a board with more digital channels could solve this disadvantage. However, the implemented solutions proved to work properly during testing. The digital output channels are used to control the motors of the locking

systems. Two outputs are used to start and to stop the motors.

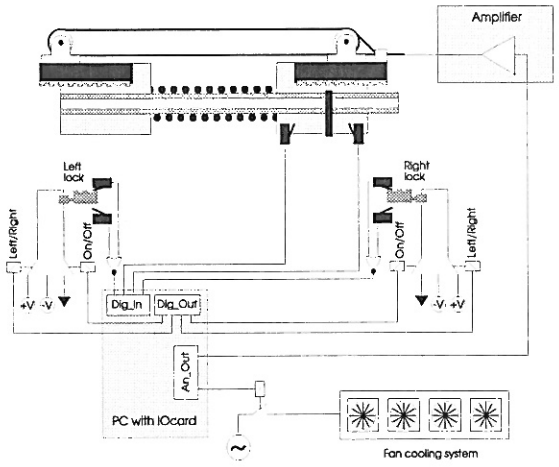

Figure 11: Simplified control scheme

The two other outputs are used to control the sense of the rotation. The analog outputs are used to operate the fan cooling system and to heat the SMA-wire through an amplifier.

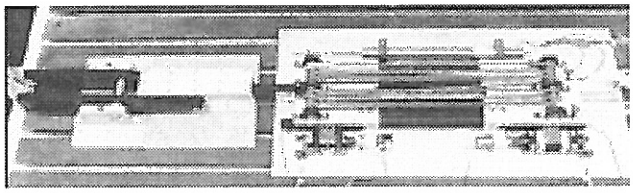

Figure 12: Overview of the experimental set-up

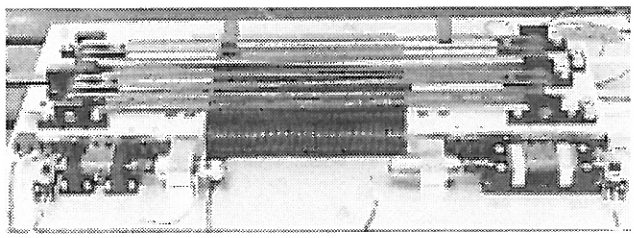

Figure 13: Detail of the inchworm actuator

During experiments, the current amplifier used to heat the SMA-wire generates an average current of 15 A. This is much less than the calculated value of 25.9 A (see chapter 5). This is due to the fact that the system is operating at room temperature and not for the specified flight conditions. The total cycle time (opening + closing) for this set-up is about 2 minutes.

6. Conclusion

This paper described the design and development of a wing flap with variable camber in order to have an optimal lift under all flight conditions. Such a variable flap reduces the fuel consumption considerably and thus enlarges the action radius of the aeroplane. In order to realise the variable camber, the trailing edge is deflected over an angle of ± 5°. Shape memory alloy (SMA) material is selected to actuate the variable flap because of its high power to mass and power to volume ratios. A stepping concept has been chosen to optimise efficiency. Possible improvements concern the locking system, which is currently overdimensioned and a further reduction of the size of the mechanism by using non-standard components.

Acknowledgment

The authors would like to thank D. Surinx, F. Bayart, and H. Voggenreiter for their contribution to this research. This research was sponsored by IWT contract INM/93/034/AMT and by the Belgian program on Inter University Attraction Poles (IUAP4-24) initiated by the Belgian State, Prime Minister's Office, Science Policy Programming. The authors assume the scientific responsibility of this paper.

References

[1] D.C. Lagoudas, I.G. Tadjbakhsh, Active flexible rods with embedded SMA fibers - Smart Materials and Structures, 162-167, Vol.1, 1992.

[2] Z. Bo, D.C. Lagoudas, Deformations and Thermal Response of Flexible Rods with Embedded SMA Actuators - Proc. of SPIE, 495-505, Vol.2190, 1994.

[3] C.H. Beahchamp, R.H. Nadolink, S.C. Dickinson, L.M. Dean, Shape memory alloy adjustable camber (SMAAC) control surfaces - 1st Eur. Conf. on Smart Structures and Materials, Glasgow, 1992.

[4] K.W. Dittrich, Formveränderung von Flügelstrukturen mittels integrierter Shape Memory Alloy Aktuatoren - Deutsche Aeospace AG, Friedrichshafen.

[5] J.S.N. Paine, C.A. Rogers, R.A. Smith, Adaptive Composite Materials with Shape Memory Alloy Actuators for Cylinders and Pressure Vessels - Proc. of SPIE, 390-401, Vol.2190, 1994.

[6] C. Rogers, D. Barker, Experimental Studies of Active Strain Energy Tuning of Adaptive Composites - 31st AIAA Structures, Structural Dynamics and Materials Conference, 2234-2241, April 1990.

[7] C.A. Rogers, C.R. Fuller, C. Liang, Active Control of Sound Radiation from Panels Using Embedded Shape Memory Alloy Fibers - Journal of Sound and Vibration, 164-170, 136(1), 1990.

[8] D. Henderson, J. Fasick, The inchworm piezoelectric stepping motor: advanced in design, performance and applications, Proc. Actuator 2000 Conf., June 2000, pp. 451-454.